Eur. Phys. J. D **34**, 73–77 (2005)
DOI: 10.1140/epjd/e2005-00122-9

THE EUROPEAN PHYSICAL JOURNAL D

Formation of fullerene dianions in a Penning trap

A. Lassesson, N. Walsh, F. Martinez, A. Herlert, G. Marx, and L. Schweikhard[a]

Institut für Physik, Ernst-Moritz-Arndt-Universität Greifswald, Domstr. 10a, 17487 Greifswald, Germany

Received 6 September 2004
Published online 13 July 2005 –

Abstract. Fullerene dianions in the range C_{70}^{2-} to C_{90}^{2-} have been created by subjecting trapped fullerene monoanions to low energy electrons in a Penning trap. The dianion production was found to be a function of the trapping-potential depth and the time of interaction between the simultaneously stored monoanions and electrons. Under similar conditions the dianion yield depends on the size of the fullerenes with more than 10% of the trapped C_{90}^{-} ions forming dianions while the corresponding relative yield for C_{70}^{2-} was less than 0.1%. The large difference can be explained by the repulsive Coulomb barrier and the second electron affinity of the fullerenes.

PACS. 36.40.-c Atomic and molecular clusters – 36.40.Wa Charged clusters

1 Introduction

In the past decade, much attention has been given to the experimental investigation and theoretical description of gas-phase multiply charged anions [1,2]. While fullerene cations have been studied extensively for various charge states [3,4], the production of fullerene dianions in the gas phase has proven to be an experimental challenge. This is due to the repulsive Coulomb barrier — a property of all multiply charged anions — that hinders electron attachment to already negatively charged species.

Fullerene dianions C_{60}^{2-} and C_{70}^{2-} were first observed in 1991 following laser desorption from a fullerene target [5,6]. These observations resulted in efforts to produce gas-phase fullerene dianions using the methods of electrospray ionisation [7–9] and electron attachment of low-energy electrons to monoanions in an ion source [10] and in ion traps [11,12]. In the latter case the production of fullerene dianions C_N^{2-}, $N = 70, 76, 86$, has been reported. More recently, dianionic fullerenes have been created through collisions between monoanions and sodium atoms [13,14].

In the present study, the technique of electron attachment to monoanions stored in a Penning trap [15] has been used to generate doubly charged fullerene anions C_N^{2-} in the range $N = 70-90$. This method has previously been applied to metal clusters [16–18], where further investigations have been performed to find the conditions for efficient dianion production [11,19]. First results on the production of dianionic fullerenes are presented and the observed relative yields are discussed with respect to the repulsive Coulomb barrier and the electron affinities.

[a] e-mail: schweikhard@physik.uni-greifswald.de

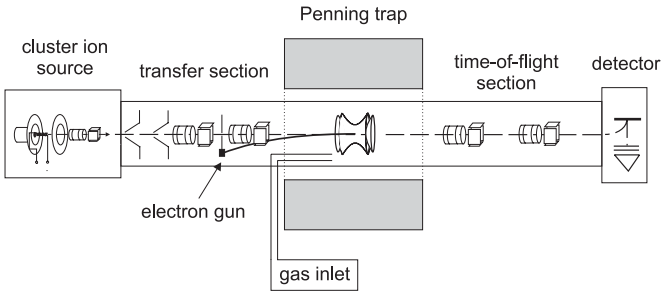

Fig. 1. Schematic drawing of the experimental set-up.

2 Experimental set-up and procedure

The ClusterTrap [20–23] consists of an ion source, a transfer section, a Penning trap within a superconducting magnet, a time-of-flight (TOF) section and a detector as shown in Figure 1. For the present study the set-up has been modified by replacing the metal-cluster laser-vaporisation source with a fullerene ion source (see Fig. 2). This source is comprised of a piece of hollow ceramic with a tungsten heating wire wound around it. A glass ampoule filled with fullerene powder (containing approximately 76% C_{60}, 22% C_{70}, and 2% higher fullerenes) is inserted. The oven is heated to 550 °C to create a molecular beam of fullerenes. A heated tungsten filament, in the shape of a spiral placed at the oven nozzle, thermionically emits electrons. As the neutral fullerenes pass through the filament, electron attachment occurs, thus creating a continuous beam of fullerene monoanions. The ions are accelerated through a set of ion optics towards the trap.

Due to the continuous ion production, the capture of the ions is somewhat different to the procedure described previously (see e.g. [23]). The ions enter the trap through

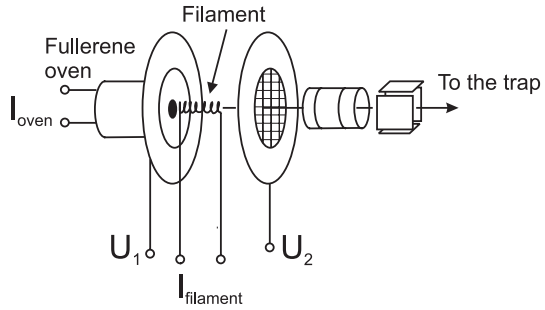

Fig. 2. Ion source for the production of fullerene monoanions. The fullerene vapour passes through a heated tungsten spiral, where electron attachment occurs. (Typical voltage differences are $U_2 - U_1 = 10$ V, typical filament heating currents are around $I = 13$ A.)

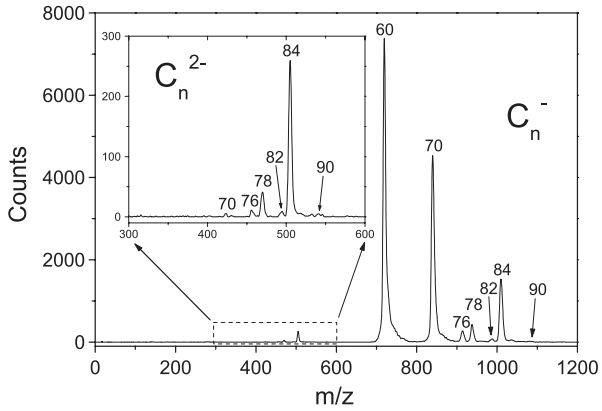

Fig. 3. TOF mass spectrum after the exposure of fullerene monoanions to an electron bath for a duration of 0.2 s and a trapping-potential depth of $U_T = 10$ V. The inset shows the mass range of fullerene dianions.

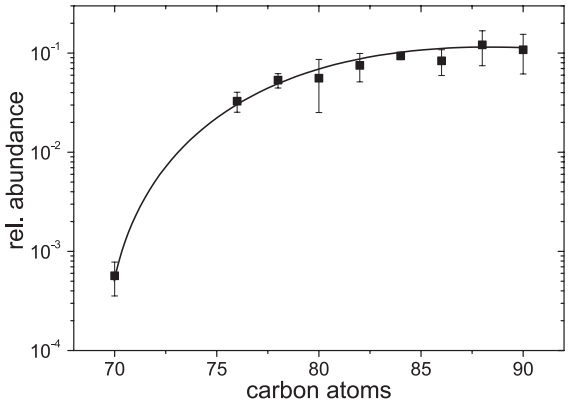

Fig. 4. Relative yield of fullerene dianions as a function of the number of atoms. The data are taken from the abundance spectrum in Figure 3. The solid line is plotted to guide the eye.

an endcap electrode with an energy slightly higher than the endcap potential, while at the same time a pulse of argon gas is applied in the trap region. Through collisions with the buffer gas some of the ions are trapped. With a simultaneous quadrupolar excitation the ions may be further centred in the trap [24]. Note, that the quadrupolar excitation enhances the capture of ions of a particular mass. However, other ions will also be trapped although not as efficiently. When enough ions have been captured, the ion beam is deflected to avoid further interaction with the stored ions.

Dianions are created by exposure of the stored monoanions to an electron bath in the Penning trap. The electron bath is composed of low energy electrons produced by ionisation of argon gas pulsed into the trap region. Ionisation of the argon gas is achieved by use of an electron beam that is guided from an external source through the trap. The electron beam is applied for a duration of 0.6 s at an energy of 40 eV with respect to the endcap potential.

After a variable reaction period, the fullerene anions are axially ejected through the second endcap and pass a TOF drift section. The ions are finally detected by single-ion counting with a conversion-electrode detector. The experimental cycle is repeated several times to increase the statistical significance of the data.

3 Results and discussion

The abundance spectrum in Figure 3 shows the result of the simultaneous trapping of fullerene monoanions and low-energy electrons. The monoanions were exposed to the electron bath for a duration of 0.2 s at a trapping-potential depth of 10 V. The most prominent peaks in the mass spectrum belong to monoanions C_{60}^-, C_{70}^-, and C_{84}^-; note that the latter ions were centred during the capture procedure. Signals that correspond to several doubly charged fullerenes are also present in the spectrum (see inset of Fig. 3). While C_{60}^{2-} has not been detected at the current settings, dianions ranging in size from C_{70}^{2-} to larger than C_{90}^{2-} are observed. In general, all fullerenes, except C_{60}, that are present in the fullerene mixture and detected as monoanions are also observed as dianions in the TOF spectrum.

While the relative intensities of the monoanion signals are in rough agreement with the relative abundances in the fullerene powder (C_{84}^- is enhanced due to the centring), the intensities of the dianions show a quite different dependence with C_{84}^{2-} as the most prominent peak. The relative yield of dianions, $C_N^{2-}/(C_N^{2-} + C_N^-)$, shows a significant size dependence (see Fig. 4). The relative abundance of C_{70}^{2-} is less than 0.1% while more than 10% of the trapped C_{90}^- monoanions are transformed into dianions.

The difference in yield between the smaller and larger fullerene dianions may be due to the Coulomb barrier, i.e. the electrostatic potential experienced by an electron approaching the monoanion. The height of the barrier will influence not only the possibility of electron attachment, but will also stabilise the highly charged anions in the case of negative second electron affinities (EA2). A dianion of a fullerene with a negative EA2 will, however, be metastable; and it can decay by tunnelling of an electron

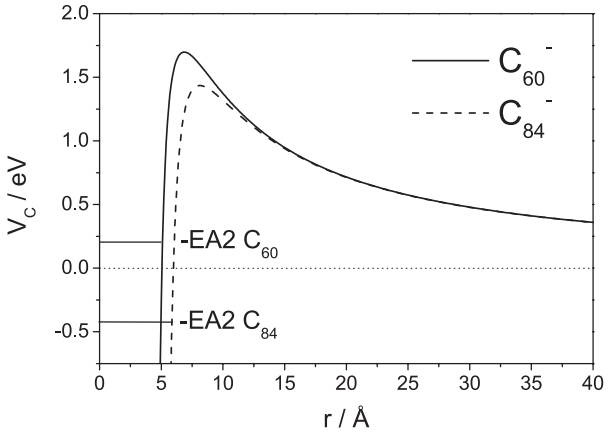

Fig. 5. Coulomb barriers for C_{60}^- and C_{84}^-. See text for details.

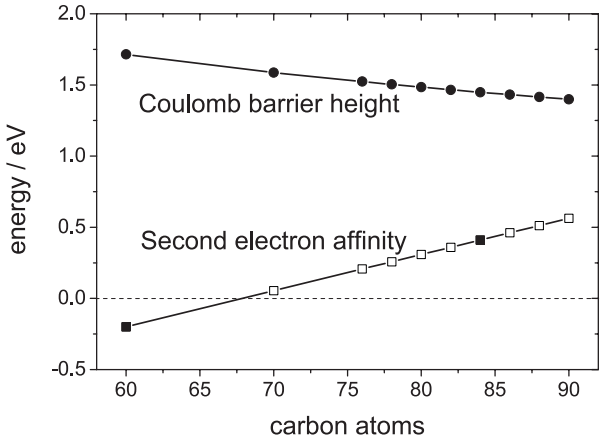

Fig. 6. Second electron affinities and Coulomb barrier heights for the investigated fullerenes and monoanions, respectively. Filled boxes are data on EA2 from the literature [9,14]. Open boxes are values from linear interpolations and extrapolations. For further details see text.

through the barrier as has recently been observed for C_{60}^{2-} [14] and smaller molecular dianions [25].

For a conducting sphere the classical form of the Coulomb barrier is given by [19,26]:

$$V_C(r,R) = \frac{e^2}{4\pi\epsilon_0}\left(\frac{|z|}{r} - \frac{R^3}{2r^2\,(r^2-R^2)}\right), \qquad (1)$$

where r is the distance to the centre of the sphere and R is its radius. z is the charge state of the sphere before the attachment of a further electron, e.g. in the present case $z=-1$ for the monoanions. In general, the most stable isomers of higher fullerenes are non-spherical. However, in first approximation the mean radius $R(N)$ of fullerenes C_N can be estimated by

$$R(N) = \sqrt{N/60}\,R(60), \qquad (2)$$

where $R(60) = 4.2$ Å is the radius of the buckminster fullerene C_{60} [13]. This relation follows from the hollow structure of fullerenes and is different to that of a compact cluster where the radius scales as the cube root of the number of atoms.

As an example, Figure 5 shows the Coulomb barriers of C_{60}^- and C_{84}^-. They are quite similar, but the potential maximum is higher for C_{60}^- than for C_{84}^- and hence it is expected that the attachment of a second electron is somewhat more likely for the latter. The height of the Coulomb barrier is given by $V_{max} = e^2/(8\pi\epsilon_0 R)$ [19] which scales inversely with the radius (see also Fig. 6). In addition, the distance of the Coulomb barrier maximum is larger for C_{84}^-, which yields a larger collisional cross-section for the electrons. Therefore, the yield of dianions is expected to increase with fullerene size as confirmed by the experimental data (Fig. 4).

Another parameter that might influence the production efficiency is the second electron affinity EA2: recent measurements indicate that EA2 is approximately -0.2 eV [14] and 0.4 eV [9] for C_{60}^{2-} and C_{84}^{2-}, respectively. Since earlier estimates have given a nearly linear relationship between the fullerene size and EA2 [8], the second electron affinity is extrapolated linearly to the other fullerenes in the respective size range $N = 60-90$ (see Fig. 6). From this assumption the EA2 value is observed to drop below zero for $N < 70$, i.e. small fullerenes allow the loss of the second surplus electron by tunnelling through the Coulomb barrier.

The half-life of C_{70}^{2-} at room temperature has been estimated to be around 80 s [8]. For C_{60}^{2-} it is even lower by orders of magnitude [14] while larger fullerenes seem, in general, to be stable when vibrationally cold (see [27] and references therein). Although the monoanions have been thermalised to room temperature in the trap, they will be excited by the attachment of a second surplus electron, i.e. heated by the relaxation of the kinetic energy of the electron into the vibrational degrees of freedom. The possibility of thermionic electron emission after heating by electron attachment has been discussed in the context of C_{76}^{2-} formation by the application of a constant beam of low-energy electrons to stored monoanions [12].

Since the sum of the second electron affinity EA2 and the Coulomb barrier height is smaller for the small fullerenes, e.g. C_{60}^{2-}, as compared to the larger fullerenes, e.g. C_{84}^{2-} (see Figs. 5 and 6), ion loss by thermionic emission is more likely to occur for the smaller fullerenes. Thus, the observed size dependence of the relative dianion yield possibly reflects a combination of an electron attachment cross-section that scales with radius and of the stability of the dianions after electron attachment. Note that similar results as those shown in Figure 4 have previously been observed in experiments on gold, silver and copper cluster dianions [19] where the relative yield dropped dramatically for clusters with a second electron affinity close to zero.

With the observation of a dependence of the dianion yield on the cluster size, the height of the repulsive Coulomb barrier, and the EA2 of the precursor fullerene, it is clear that efficient production of dianions in the ClusterTrap apparatus is influenced by the properties of the electron bath to which the monoanions are exposed. For attachment of a further surplus electron to a

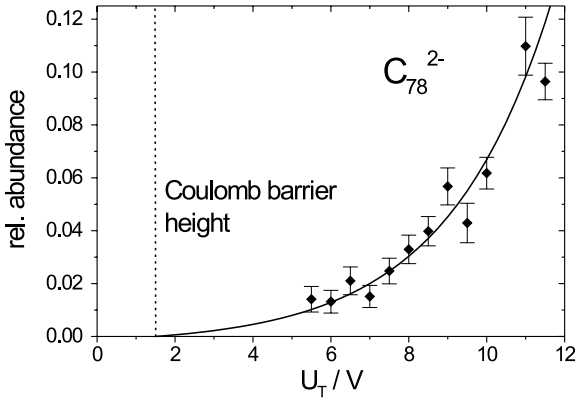

Fig. 7. The relative yield of C_{78}^{2-} as a function of trapping-potential depth U_T. The solid line is an exponential fit to the data to guide the eye.

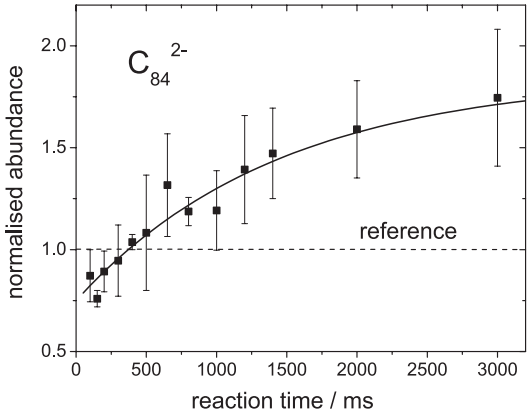

Fig. 8. Relative yield of C_{84}^{2-} as a function of the reaction time in the electron bath at a trapping-potential depth of $U_T = 10$ V. The data points are the average of two different measurements. They are normalised to the result of a measurement at a fixed reaction time recorded quasisimultaneously in alternation to the measurements taken for variable times [21]. The solid line is a fit to the data as described in the text.

monoanion, the electron must have enough energy to overcome the Coulomb barrier. The maximum kinetic energy possible for a trapped electron is limited by the magnitude of the electrostatic quadrupolar potential [28] in the axial direction

$$U(z) = \frac{U_0}{2d_0^2} z^2, \tag{3}$$

where U_0 is the potential difference between the ring and endcap electrodes and d_0 is the trap dimension defined as $d_0^2 = (z_0^2 + r_0^2/2)/2$ with r_0 and z_0 as the radial and axial distance of the electrodes to the centre of the trap. The trapping depth is given by $U_T = U(z_0) - U(0) = U_0(z_0^2/(2d_0^2))$, where for the given hyperbolical geometry of the asymptotically symmetric Penning trap [29], i.e. $d_0^2 = z_0^2$, it simplifies to $U_T = U_0/2$. Only a fraction of electrons have energies large enough to overcome the electrostatic repulsion. The deeper the trapping-potential depth, U_T, the larger the initial energy of the electrons and the more likely they can overcome the Coulomb barrier of the monoanion in order to attach.

The influence of the trapping-potential on the production of fullerene dianions has been investigated in the case of C_{78}^{2-} (Fig. 7). These measurements were performed for a fixed reaction time of 0.5 s in the electron bath. The data plotted in Figure 7 show an increase of the relative dianion yield as a function of the trapping-potential depth U_T. As the lowering of U_T influenced not only the dianion production, but also the trapping efficiency for monoanions, it was not possible to achieve sufficient ion intensities below 5.5 eV for the present experimental settings. To guide the eye, the data points are fitted with an exponentially increasing function that is zero at the maximum value of the C_{78}^- Coulomb barrier (Eq. (1)). The observed behaviour is in agreement with previous measurements for Au_{25}^{2-} and C_{70}^{2-} [11] where a similar increase in the relative yield was observed for an increase in U_T.

Further investigations involved the determination of the dependence of the dianion production on the reaction time of the monoanions in the electron bath. C_{84}^{2-} dianions were created by simultaneous storage of the monoanions with the low-energy electrons for variable reaction times. The corresponding relative dianion yield is plotted in Figure 8. It increases with reaction time and saturates for times larger than about 2 s. A significant fraction of the dianions, approximately 40% of the yield in saturation, are created during the application of the electron beam (600 ms). In order to guide the eye, a growth function $I(t) = I_1(1 - 2^{-t/\tau}) + I(0)$ was fitted to the data in Figure 8 which yields a time constant $\tau = 1.0$ s.

This behaviour is similar to that previously observed for the production of Au_{27}^{2-} [19] under similar conditions. The initial increase in the dianion yield suggests that a longer storage time allows for a higher probability of electron attachment. The observed saturation of the signal is considered to be due to a decrease in energy of the stored electrons below the Coulomb barrier height, since the trapped electrons may lose their kinetic energy by synchrotron radiation [28,30] and/or collisions with both the buffer gas and the stored ions. It is not due to ion loss as after a few seconds still almost 90% of the fullerenes are monoanionic.

4 Conclusion and outlook

Fullerene dianions have been created over a broad size range by exposure of monoanions to a low-energy electron bath in a Penning trap. The dianion yield is highly size-dependent with over 10% of the trapped C_{90}^- forming dianions, while no C_{60}^{2-} has been observed for the present experimental settings. The large difference in the relative yield between smaller and larger dianions can be attributed to the corresponding repulsive Coulomb barriers of the monoanions and the second electron affinities of the fullerenes.

The change of the relative dianion yield by the variation of the trapping-potential depth, and hence of the electron energy, indicates the influence of the Coulomb

barrier on the electron attachment process. The dianion yield could be improved by increasing the interaction time of electrons and monoanions in the trap. This is, however, limited by energy loss of the electrons.

As the dianions are expected to be excited in the electron attachment process it might be necessary to apply a cooling, i.e. a deexcitation, during the electron bath in order to enhance the yield of the smaller dianions. Possibly, a buffer gas can be used to this end. Thus, the method of dianion production with an electron bath in a Penning trap which has been applied in this work may also be extended to smaller fullerenes as e.g. to C_{60}. The use of other fullerene mixtures or ion sources should also lead to the production of larger fullerene dianions and possibly also trianions. This will enable the investigation of photo-excited and collisionally activated dianions over a wide range of fullerene sizes.

Financial support from the EU Cluster Cooling Network (IHP-CT-2000-00026) is gratefully acknowledged. The experiments have been performed at the Max Planck Institute for Plasma Physics (IPP) at Greifswald. We thank the IPP for its kind hospitality and support.

References

1. M.K. Scheller, R.N. Compton, L.S. Cederbaum, Science **270**, 1160 (1995)
2. A. Dreuw, L.S. Cederbaum, Chem. Rev. **102**, 181 (2002)
3. P. Scheier, B. Dünser, R. Wörgötter, M. Lezius, R. Robl, T.D. Märk, Int. J. Mass Spectrom. **138**, 77 (1994)
4. V.R. Bhardwaj, P.B. Corkum, D.M. Rayner, Phys. Rev. Lett. **91**, 203004 (2003)
5. R.L. Hettich, R.N. Compton, R.H. Ritchie, Phys. Rev. Lett. **67**, 1242 (1991)
6. P.A. Limbach, L. Schweikhard, K.A. Cowen, M.T. McDermott, A.G. Marshall, J.V. Coe, J. Am. Chem. Soc. **113**, 6795 (1991)
7. G. Khairallah, J.B. Peel, Chem. Phys. Lett. **296**, 545 (1998)
8. O. Hampe, M. Neumaier, M.N. Blom, M.M. Kappes, Chem. Phys. Lett. **354**, 303 (2002)
9. O.T. Ehrler, J.M. Weber, F. Furche, M.M. Kappes, Phys. Rev. Lett. **91**, 113006 (2003)
10. R.N. Compton, A.A. Tuinman, C.E. Klots, M.R. Pederson, D.C. Patton, Phys. Rev. Lett. **78**, 4367 (1997)
11. A. Herlert, R. Jertz, J. Alonso Otamendi, A.J. González Martinez, L. Schweikhard, Int. J. Mass Spectrom. **218**, 217 (2002)
12. J. Hartig, M.N. Blom, O. Hampe, M.M. Kappes, Int. J. Mass Spectrom. **229**, 93 (2003)
13. B. Liu, P. Hvelplund, S. Brøndsted Nielsen, S. Tomita, Phys. Rev. Lett. **92**, 168301 (2004)
14. J.U. Andersen et al., Private communication
15. A. Herlert, S. Krückeberg, L. Schweikhard, M. Vogel, C. Walther, Phys. Scripta **T80**, 200 (1999)
16. L. Schweikhard, A. Herlert, S. Krückeberg, M. Vogel, C. Walther, Philos. Mag. B **79**, 1343 (1999)
17. A. Herlert, L. Schweikhard, M. Vogel, Eur. Phys. J. D **16**, 65 (2001)
18. C. Yannouleas, U. Landman, A. Herlert, L. Schweikhard, Phys. Rev. Lett. **86**, 2996 (2001)
19. A. Herlert, L. Schweikhard, Int. J. Mass Spectrom. **229**, 19 (2003)
20. S. Becker, K. Dasgupta, G. Dietrich, H.-J. Kluge, S. Kuznetsov, M. Lindinger, K. Lützenkirchen, L. Schweikhard, J. Ziegler, Rev. Sci. Instrum. **66**, 4902 (2003)
21. L. Schweikhard, St. Becker, K. Dasgupta, G. Dietrich, H.-J. Kluge, D. Kreisle, S. Krückeberg, S. Kuznetsov, K. Lindinger, K. Lützenkirchen, B. Obst, C. Walther, H. Weidele, J. Ziegler, Phys. Scripta **T59**, 236 (1995)
22. L. Schweikhard, S. Krückeberg, K. Lützenkirchen, C. Walther, Eur. Phys. J. D **9**, 15 (1999)
23. L. Schweikhard, K. Hansen, A. Herlert, G. Marx, M. Vogel, Eur. Phys. J. D **24**, 137 (2003)
24. G. Savard, St. Becker, G. Bollen, H.-J. Kluge, R.B. Moore, Th. Otto, L. Schweikhard, H. Stolzenberg, U. Wiess, Phys. Lett. A **158**, 247 (1991)
25. P. Weis, O. Hampe, S. Gilb, M.M. Kappes, Chem. Phys. Lett. **321**, 426 (2000)
26. J.D. Jackson, *Classical Electrodynamics*, 3rd edn. (Wiley, New York, 1999)
27. Q. Shi, S. Kais, Mol. Phys. **100**, 475 (2002)
28. L.S. Brown, G. Gabrielse, Rev. Mod. Phys. **58**, 233 (1986)
29. R.D. Knight, Int. J. Mass Spectrom. Ion Proc. **51**, 127 (1983)
30. L. Schweikhard, A. Herlert, G. Marx, *Simultaneous Trapping of Electrons and Anionic Clusters in a Penning Trap*, in "NON-NEUTRAL PLASMA PHYSICS V: Workshop on Non-Neutral Plasmas" (Santa Fe, New Mexico, July 2003), edited by M. Schauer, T. Mitchell, R. Nebel, AIP Conf. Proc. **692**, 203 (2003)